Liu *et al.*
Chinese Journal of Mechanical Engineering (2022) 35:133
https://doi.org/10.1186/s10033-022-00806-0

Chinese Journal of Mechanical Engineering

ORIGINAL ARTICLE

Open Access

Feasibility Study of the GST-SVD in Extracting the Fault Feature of Rolling Bearing under Variable Conditions

Xiangnan Liu[1], Xuezhi Zhao[1] and Kuanfang He[2*]

Abstract

Feature information extraction is one of the key steps in prognostics and health management of rotating machinery. In the present study, an investigation about the feasibility of a methodology based on generalized S transform (GST) and singular value decomposition (SVD) methods for feature extraction in rolling bearing, due to local damage under variable conditions, is conducted. The technique adopts the GST method, following the time-frequency analysis, to transform a raw fault signal of the rolling bearing into a two-dimensional complex matrix. And then, the SVD method is performed to decompose the matrix to obtain the feature vectors. By this procedure it is possible to obtain the fault feature information of rolling bearing under different speeds and different loads. In order to streamline the feature parameters of the feature vectors to train more uncomplicated models, the principal component analysis (PCA) subsequently performed. The particle swarm optimization-support vector machine (PSO-SVM) model is used to identify and classify the different fault states of rolling bearing. Furthermore, in order to highlight the superiority of the proposed method some comparisons are conducted with the conventional methods. The obtained results show that the proposed method can effectively extract fault features of the rolling bearing under variable conditions.

Keywords: Feature extraction, Generalized Stockwell transform, Singular value decomposition, Principal component analysis

1 Introduction

The fault feature extraction of rolling bearing is a research topic of great interest for the prognostics and health management (PHM) rotating machinery. It is due to local damages that causes vibration impacts, between the structures of the rolling bearing. Generally, operating environment of the rotating machines is complex with a large disturbance which has a remarkable adverse impact on the machine performance. Studies show that such an environment can make local damages on the rolling bearing [1]. Once the rolling bearing fails, it will cause serious economic losses and even causalities. Therefore, conducting a fault diagnosis for the rolling bearing is of significant importance, which has attracted many scholars in recent years [2].

The vibration signal collected by the sensor contains a large amount of operating states information of rolling bearing. It was found that analyzing the vibration signal can effectively realize the feature extraction of the rolling bearing [3]. The conventional methods for analyzing the vibration signal of rolling bearing often assume that the operating condition is stable [4]. Due to the complicated structure of rotating machinery, rolling bearings are usually operated under variable conditions [5]. The vibration signal collected from rolling bearing under variable conditions can reflect the weak fault feature well. Therefore, the conventional fault feature extraction methods based on the assumption of stable operating condition are inevitably limited [6]. Although finding an effective vibration

*Correspondence: hkf791113@163.com

[2] School of Mechatronic Engineering and Automation, Foshan University, Foshan 528225, China
Full list of author information is available at the end of the article

signal processing method is of significant importance for rotating machinery from prognostics and health management (PHM) viewpoint, fault feature of the rolling bearing under variable conditions can be hardly extracted by conventional methods for analyzing the vibration signal [7].

It is worth noting that the vibration signal of the rolling bearing is non-stationary, which originates from its complex structure [8]. In spite of superior characteristics of the conventional Fourier transform method, it has shortcomings in analyzing the vibration signal, including challenges in the time and frequency localization. Time frequency analysis (TFA) method can provide the joint distribution information. Therefore TFA method is an appropriate scheme for analyzing the vibration signal of the rolling bearing. Several popular TFA methods including the short time Fourier transform (STFT) [9], continuous wavelet transform (CWT) [10] and Stockwell transform (S-transform) [11], have been proposed so far for processing the fault vibration signal of the rolling bearing.

STFT is a very powerful tool for processing the non-stationary signals. The overall time-frequency trend of the signal can be obtained by STFT method. However, the STFT method still has some challenges in engineering applications. More specifically, when the STFT method is applied to process the time frequency distribution of the raw signal, high time and frequency resolution cannot be obtained simultaneously [12]. This is mainly attributed to the limitations in the window function of the STFT method.

CWT, which has the characteristic of providing good time-frequency localization for the non-linear and non-stationary signals. It has been widely used to conduct an analyzing for the rolling bearing. Although the CWT method has variable window function, the selection of its basis function does not have reasonable adaptability. Accordingly, applying the CWT method to obtain the time frequency distribution of the raw signal has some disadvantages, such as border distortion, energy leakage and interference terms [13–15].

S transform, another time frequency analysis method, was proposed by Stockwell in 2002 [16]. The S transform method maintains the absolute phase information of the signal and provides a variable signal decomposition scale. Therefore, it can be regarded as an extension for the STFT and CWT methods [17]. Moreover, the S transform method is a reversible TFA method and its time frequency resolution changes with the frequency [18]. However, the basic wavelet of the S transform method is fixed, which cause some disadvantages in engineering applications, such as insufficient time frequency resolution regulation and insufficient energy aggregation [19, 20].

Aiming at resolving shortcomings of the above mentioned TFA methods, the generalized S transform (GST) method has been proposed by Pinnegar. The GST method has gained remarkable popularity among researchers [21]. The GST method can automatically adjust the width of the window function and has been widely used to analyze the vibration signal of the rolling bearing [22]. In the present study, the superiority of GST over S transform will be shown in detail. Based on the above analysis, the GST method is adopt to extract the fault feature information of rolling bearing under variable conditions. Although the feature information can be extracted by GST, the two-dimensional complex matrix obtained from GST is too large to be regard as the fault feature vectors.

Singular value decomposition (SVD) has good stability and is an inherent characteristic of the matrix, which can fully reflect the feature information contained in the complex matrix with favorable stability [23, 24]. So, the SVD method is performed to the complex matrix to obtain the feature vectors. In engineering applications, the feature vectors obtained from SVD method contains a lot of feature information, which complicates the extraction of fault features of the rolling bearing [25]. Thus, obtaining the concise feature parameters is a significant issue in the SVD method. In order to obtain more concise feature parameters, the principal component analysis (PCA) method is introduced to conduct a data compression for the feature vectors.

After extracting feature parameters, the states recognition of rolling bearing is another significant issue for condition monitoring of rotating machinery. Support vector machine (SVM), as an intelligent technology, has been widely applied to identify fault states in diverse practical applications [17]. However, one of the main challenges of the SVM method is determining the values of the penalty factor and kernel function parameters [26]. Recently, the Particle Swarm Optimization (PSO) algorithm has been proposed, which is suitable for determining the values of the penalty factor and kernel function parameters [27, 28].

Compared to the existing studies, the main objectives and contributions of this research are as follows: (1) A new time-frequency feature extraction scheme is proposed for the feature extraction of rolling bearing under different speeds and different loads. (2) The influence of the window function parameters of GST on the time-frequency feature extraction are analyzed according to the numerical simulations. (3) The superiority of GST in feature extraction of rolling bearing is studied. (4) The

PSO-SVM model with different feature extraction methods are employed for comparison.

The framework of this article is arranged as follows: the theoretical basis of the GST, SVD, PCA and PSO-SVM model are introduced in Section 2. Then the proposed methods are described in Section 3. Moreover, the simulated and experimental data are analyzed in Section 4 and Section 5, respectively. Finally, conclusions are summarized in Section 6.

2 Methodology

2.1 Generalized S Transform

The GST is an extension of the standard S transform and can be derived from a STFT based on a Gaussian window function. The STFT of one-dimensional continuous signal $x(t)$ is defined as

$$STFT_x(\tau,f) = \int_{-\infty}^{\infty} x(t)g(t-\tau)e^{-j2\pi ft}\mathrm{d}t, \tag{1}$$

where f and t represent the frequency and the time, respectively. Moreover, $g(t)$ and τ denote the Gaussian window function and the position of the $g(t)$ on the time axis

When the $g(t)$ is defined as a Gaussian window function

$$g(t) = \frac{1}{\sigma\sqrt{2\pi}}e{-}t^2\Big/2\sigma^2, \tag{2}$$

and the scale factor σ is defined as

$$\sigma{=}1\big/|f|. \tag{3}$$

It is obvious that

$$\int_{-\infty}^{+\infty} \frac{|f|}{\sqrt{2\pi}}e^{-(t-\tau)^2f^2/2}\mathrm{d}\tau = 1. \tag{4}$$

Then the standard S transform of signal $x(t)$ can be obtained by combining Eqs. (1, 2, 3 and 4):

$$S_x(\tau,f) = \int_{-\infty}^{+\infty} x(t)\frac{|f|}{\sqrt{2\pi}}e^{-(t-\tau)^2f^2/2}e^{-j2\pi ft}\mathrm{d}\tau. \tag{5}$$

It is worth noting that the scale factor σ of a Gaussian window is inversely proportional to the frequency. Although the standard S-transform has been applied in some fields, one of its main disadvantages is that the basic wavelet shape is fixed. Therefore, it cannot be adjusted in accordance with the requirements of the specific application. This shortcoming has a significant negative influence on the adaptability of the standard S-transform for the signal analysis [19].

In order to overcome the disadvantages of standard S transform, Pinnegar et al. [21] applied one adjustable parameters p on the standard S-transform and proposed the GST scheme, accordingly. The GST scheme for the signal $x(t)$ is defined as:

$$GST_x^p(\tau,f) = \int_{-\infty}^{+\infty} x(t)\frac{|f|^p}{\sqrt{2\pi}}e^{-(t-\tau)^2f^2/2}e^{-j2\pi ft}\mathrm{d}\tau, \tag{6}$$

where, $\sigma = 1/|f|^p$, p is an adjustment parameter, and $0<p\leq 1$ [29]. When p=1, Eq. (6) is equal to Eq. (5). For a discrete signal $x(n)$, Eq. (6) can be expressed as

$$GST_x^p\left(iT,\frac{n}{NT}\right) = \sum_{m=1}^{N} X\left(\frac{n+m}{NT}\right)e^{\frac{-2n^2m^2}{n^{2p}}}e^{\frac{j2\pi mi}{N}}, \tag{7}$$

$$GST_x^p(iT,0) = \frac{1}{N}\sum_{m=1}^{N} X\left(\frac{m}{NT}\right), \tag{8}$$

where N and T denote the total sampling point and the sampling interval of the signal, respectively. Moreover $X\left(n/NT\right)$ is the discrete time sequence of the signal $x(t)$ and $i,n = 1,2,\cdots,N$.

According to Eqs. (7) and (8), the GST method can transform the one-dimensional raw signal into a two-dimensional complex matrix in the form below:

$$GST_{m\times n} = \boldsymbol{A}_{m\times n}e^{j\boldsymbol{\theta}_{m\times n}}, \tag{9}$$

where $\boldsymbol{A}_{m\times n}$ and $\boldsymbol{\theta}_{m\times n}$ are the amplitude matrix and the phase matrix, respectively.

In addition, according to Eq. (6), the GST model can effectively change the Gaussian window width by adjusting the parameter p. Then the improved time- frequency resolution and time-frequency aggregation performance can be obtained. Therefore, the time- frequency aggregation performance of the GST depends on the selection of the parameter p. Stankovic [30] proposed an energy concentration measure criterion for measuring the time-frequency distribution. The proposed criterion is defined as:

$$M_x(p) = \left[\int_{-\infty}^{\infty}\int_{-\infty}^{\infty}\left|GST_x^p(\tau,f)\right|^{1/q}\mathrm{d}\tau\,\mathrm{d}f\right]^q, \tag{10}$$

The discrete form of Eq. (10) is defined as

$$M_x(p) = \left[\sum_{n=1}^{N}\sum_{k=1}^{N}\left|GST_x^p(n,k)\right|^{1/q}\right]^q, \tag{11}$$

where $\sum_{n=1}^{N}\sum_{k=1}^{N} GST_x(n,k) = 1$ is the energy normalized constraint of GST coefficient, and q>1. According to the above evaluation criteria, the GST with optimization time-frequency aggregation performance is designed. The calculation steps are as follows.

(1) For $p \in (0, 1]$, perform a GST on the signal $x(t)$ using Eq. (6).
(2) Normalized the energy of the calculated GST:

$$GST_x^p(n,k) = \frac{GST_x^p(n,k)}{\sum_{n=1}^{N}\sum_{k=1}^{N} GST_x^p(n,k)}. \quad (12)$$

(3) Calculate the time-frequency aggregation according to Eq. (10), and $q = 2$.
(4) The optimal value of parameter p can be calculated by Eq. (13)

$$P_{opt} = \min_p [M_x(p)]. \quad (13)$$

2.2 Principle of SVD

The real matrix $\boldsymbol{A} \in R^{m\times n}$ can be decomposed by the SVD as the following [31]:

$$\boldsymbol{A}_{m\times n} = \boldsymbol{USV}^{\mathrm{T}}, \quad (14)$$

where $\boldsymbol{U} \in R^{m\times m}$, $\boldsymbol{V} \in R^{n\times n}$, $\boldsymbol{U}$ and $\boldsymbol{V}$ are the orthogonal matrix, while $\boldsymbol{S}$ is a diagonal matrix, which can be expressed as $\boldsymbol{S}$=[diag (σ_1, σ_2, ..., σ_k), $\boldsymbol{O}$], $\boldsymbol{O}$ is the zero matrix, k=min(m, n), $\sigma_1 \geq \sigma_2 \geq \cdots \geq \sigma_k > 0$.

It is generally believed that the feature information in the amplitude matrix is mainly concentrated on the first r effective singular values, and the turning point of the singular value is fixed when it changes rapidly to be gentle and smooth. The corresponding ordinal number of this point is valid values r [32].

More details about the SVD can be found in Ref. [31].

2.3 The Basic Theory of PCA

PCA is a commonly used method to reduce the signal from high-dimensional data space to low-dimensional data space [33]. The main steps of PCA is defined as

$\boldsymbol{X}$= $[x_0, x_1, \ldots, x_{N-1}]^{\mathrm{T}}$ are the components of the signal $x(t)$ processed by GST and SVD, $\boldsymbol{x}_i = [\sigma_1, \sigma_2, \cdots, \sigma_r]$, $i =$ 0, 1, ... , N−1, the mean of the samples can be calculated by Eq. (15):

$$\overline{x} = \frac{1}{N}\sum_{i=0}^{N-1} x_i. \quad (15)$$

According to Eq. (15), the co-variance matrix $\boldsymbol{S}_x$ of X is defined as

$$\boldsymbol{S}_x = \frac{1}{N}\sum_{i=0}^{N-1}\left[(x_i - \overline{x})(x_i - \overline{x})^{\mathrm{T}}\right]. \quad (16)$$

The $(\lambda_1, \lambda_2, \cdots, \lambda_r)$ is defined as the eigenvalues of the co-variance matrix $\boldsymbol{S}_x$, and $\lambda_1 \geq \lambda_2 \geq \cdots \geq \lambda_r$. The corresponding feature vector is defined as u_l, l = 1, 2, ... , r. Thus, all eigenvalues can form an orthogonal matrix $\boldsymbol{U} = [u_1, u_2, \cdots, u_r]$.

The cumulative variance contribution rate can be used to measure the information representation of the new generated components to the original data. In practical applications, the principal component is usually selected according to the cumulative percent variance (CPV). The CPV is defined as

$$CPV = \sum_{i=1}^{k}\lambda_i \Big/ \sum_{i=1}^{r}\lambda_i. \quad (17)$$

It is generally believed that the current k principals can over more original data information when CPV≥0.95 [34]. The orthogonal matrix composed of the first k eigenvalues is used as the low-dimensional projection space $\boldsymbol{U}_k = [u_1, u_2, \cdots, u_k]$, and the original data can be reduced from r-dimensional to k-dimensional. The feature parameter matrix $\boldsymbol{Y}_{n\times k}$ obtained by PCA can be calculated as

$$\boldsymbol{Y}_{n\times k} = \boldsymbol{X}_{n\times r}\boldsymbol{U}_{r\times k}. \quad (18)$$

2.4 PSO-SVM Model

SVM is especially suitable for data processing of small samples due to its unique advantage. However, the values of the penalty factor and kernel function parameters of SVM model have an important influence on its learning ability and generalization ability. The PSO algorithm is used to optimize the parameters of the SVM model in this paper. The details about the SVM and PSO can be found in Refs. [26–28]. The flowchart of PSO-SVM model is shown in Figure 1.

3 Fault Diagnosis Method Based on PSO- SVM

In this section, it is intended to propose a new scheme for extracting fault features of rolling element bearings under variable conditions. To this end, GST, SVD and PCA methods are utilized. A framework of the proposed algorithm is presented in Figure 2.

The steps of the proposed method are as follows:

Step 1: The time-frequency domain transform of each raw signal is conducted by using GST, and the amplitude matrix of GST is used as feature matrix.
Step 2: The SVD is performed to the feature matrix to obtain the feature vectors, which are composed of multiple sets of singular value.
Step 3: The PCA is subsequently performed to the feature vectors to extract the more streamlined feature parameters for accurate fault classification.
Step 4: The PSO-SVM model is introduced for identification and classification of different bearing typi-

cal faults, and a comparison is made among different feature extraction methods and different models.

4 Simulation Analysis

In order to evaluate the performance of the GST, a simulated signal is constructed. The numerical model is defined as

$$x(t) = e^{(-400t_1)}\sin(2\pi f_1 t) + \sin(2\pi f_2 t) + 0.8\sin(2\pi f_3 t) + \sin(2\pi f_4 t) + r(t), \quad (19)$$

where $t_1 = mod(t,1/33)$, the fault feature frequency of the impact signal is $f_0 = 33$ Hz, *mod* is the remainder function, $f_1 = 3500$ Hz, $f_2 = 450$ Hz, $f_3 = 150$ Hz, $f_4 = 48$ Hz, $r(t)$ is Gaussian white noise and $r(t) \sim N(0, 0.16)$.

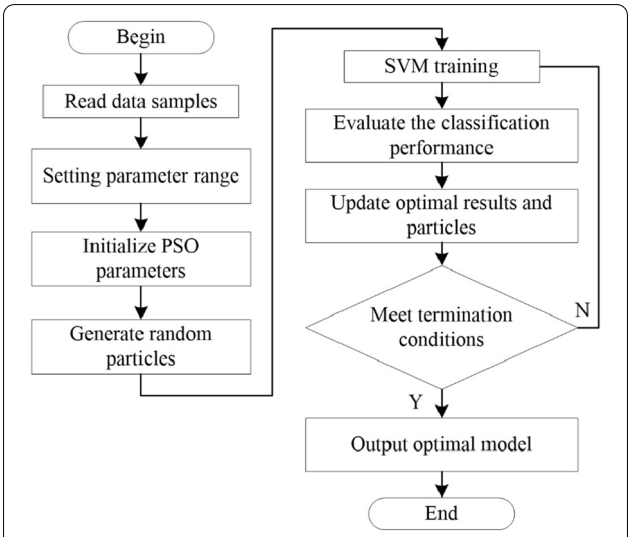

Figure 1 Flowchart of PSO-SVM model

The sampling frequency and the data length of the simulated signal are 8 kHz and 4000 point, respectively. Figure 3(a) shows the waveform of signal $x(t)$. The time-frequency distribution of simulated signal obtained by STFT and CWT are shown in Figure 3(b–c), respectively. The GST of simulated signal $x(t)$ with different values of parameter p ($p = 0.7$, 0.8, and 1.0) are shown in Figure 3(d)–(f), respectively.

As shown in Figure 3(b), the time-frequency representation obtained by STFT can detect the low frequency component (f_2, f_3, f_4) clearly. However, the concentration of high frequency component (f_1) is not well. In addition, the energy distribution of the impact signal is completely misrepresent due to the deficient time resolution of the STFT. Although the impact feature information of the simulated signal can be identified from Figure 3(c), the concentration of frequency component (f_0), which corresponding to the time interval 0.03 s is very poor. Otherwise, the time-frequency distribution of frequency component (f_2, f_3, f_4) is well.

The time-frequency representation of GST with $p = 0.6$ is plotted in Figure 3(d). It can be seen that the frequency component (f_2, f_3, f_4) can be detect clearly. Moreover, the frequency component (f_0), which corresponding to the time interval 0.03 s has a good frequency domain resolution, but its time domain resolution is poor. The standard S transform (where $p = 1.0$) of simulated signal is plotted in Figure 3(e). It can be seen that only the frequency component (f_3, f_4) can be detect clearly. The time-frequency distribution of frequency component (f_2) is not well. In addition, the frequency component (f_0), which corresponding to the time interval 0.03 s has a good time domain, but its frequency domain resolution is poor.

The optimal GST with $p_{opt} = 0.8$ is plotted in Figure 3(f). The time-frequency representation obtained by

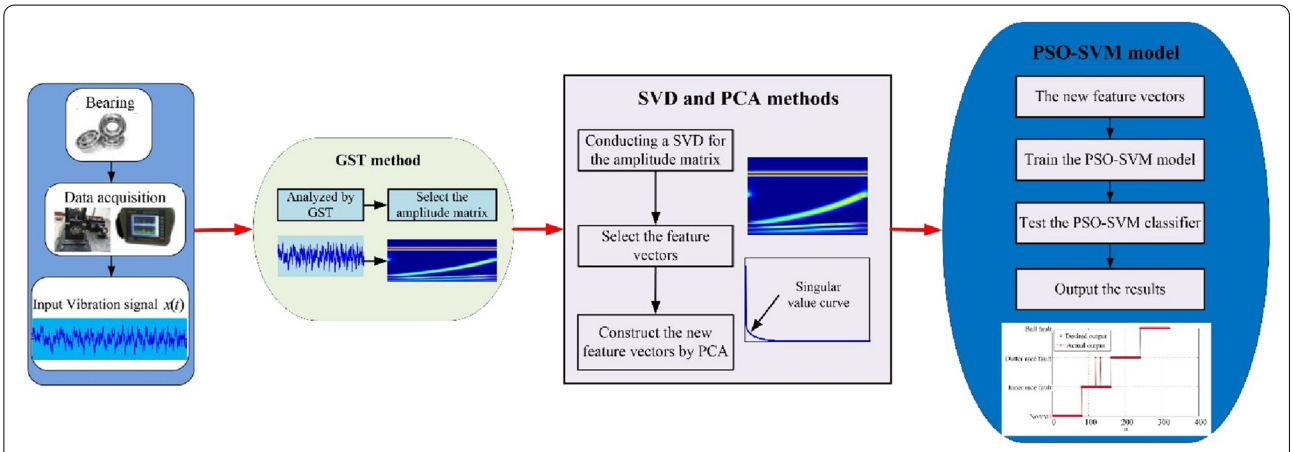

Figure 2 Framework of the proposed algorithm

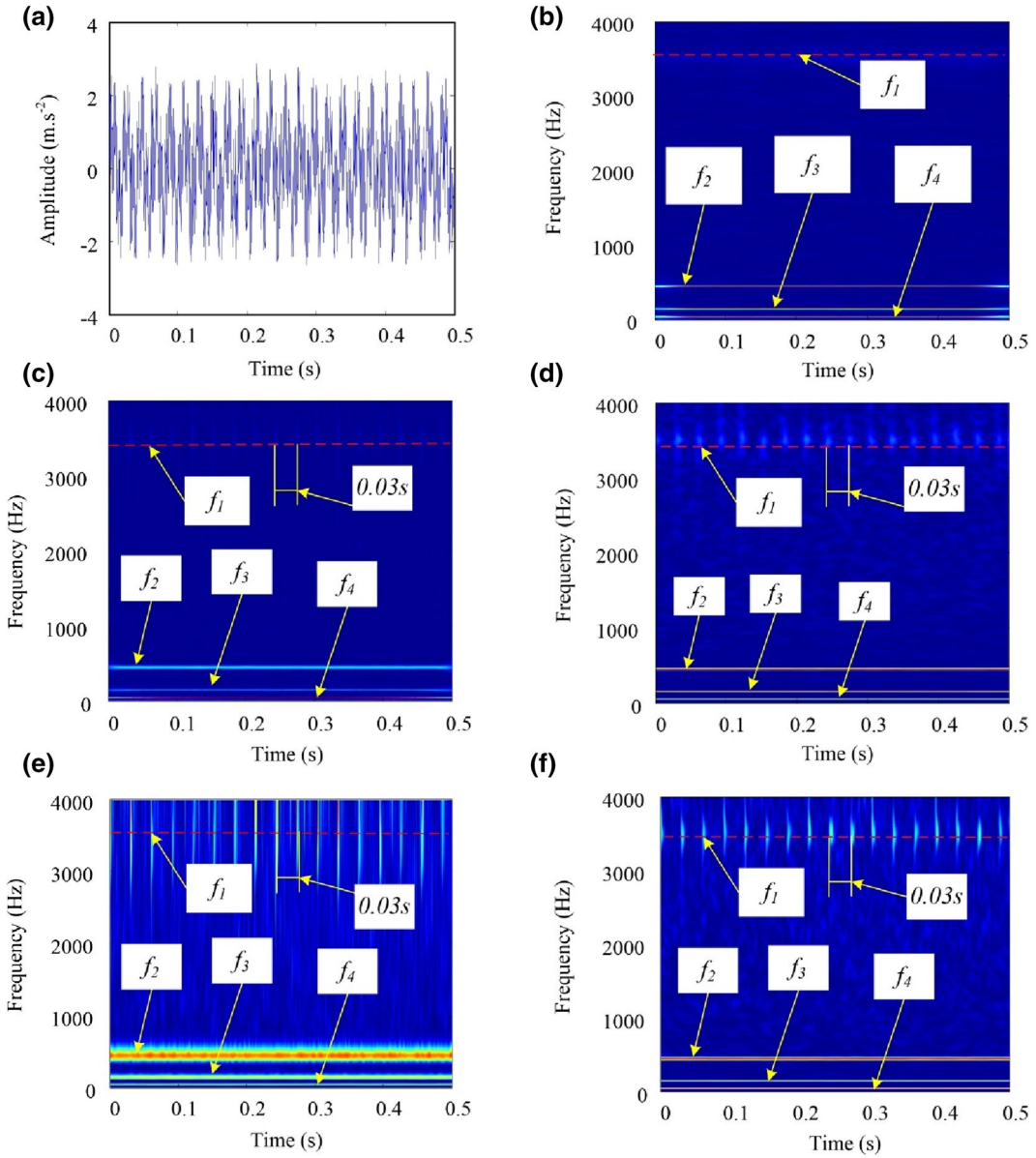

Figure 3 Waveform of simulated signal and its time-frequency spectra: (**a**) time domain waveform, (**b**) STFT, (**c**) CWT, (**d**) GST with $p = 0.6$, (**e**) GST with $p = 1$, (f) GST with $p_{opt} = 0.8$

optimal GST can detect all frequency components. The energy distribution of impact signal is more satisfactory than other techniques.

Based on the above analysis, the time-frequency energy concentration obtained by the optimal GST has a great improvement than the standard S transform, STFT and CWT.

5 Experimental Analysis

5.1 Experiment Data Sources

In this section, an experiment data collected from Case Western Reserve University are adopted to conduct an analysis [35]. The experiment data has been widely used in many researches and has been proved to be effective in the verification of rolling bearing feature extraction methods [36]. The main equipment and instruments of the bench experimental platform comprise the dynamometer, torque meter and displayer, coupling,

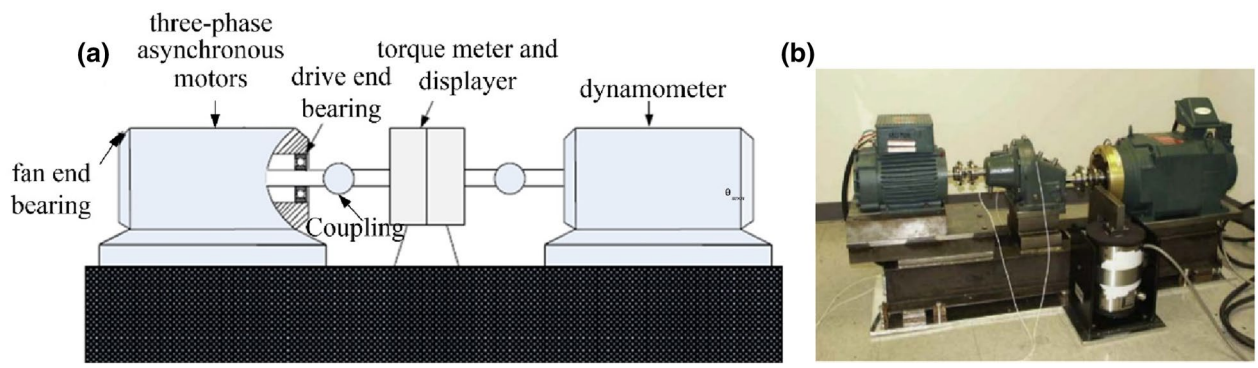

Figure 4 Schematic diagram and physical map of the experiments platform: (**a**) schematic diagram, (**b**) physical map

Table 1 Parameters of 6205-2RS JEM SKF

Parameter	Outer diameter (mm)	Inner diameter (mm)	Thickness (mm)	Rolling element diameter (mm)	Number of rollers
Value	52	25	15	7.94	9

drive end bearing, three-phase asynchronous motors, and fan end bearing, as shown in Figure 4.

Vibration signal of rolling bearing in four typical states of the normal, inner ring fault (IRF), outer ring fault (ORF) and body fault (BF) are tested in the experiment. The type of rolling bearing is 6205-2RS JEM SKF. Table 1 lists the parameters of the rolling bearing.

In the manufacturing process of bearing fault parts, a single-point fault with a diameter of (0.1788 mm, 0.3576 mm, 0.5364 mm, 0.7152 mm) are processed on the surface of the bearing inner ring, outer ring and body by electric spark technology, respectively. The accelerometer was placed at the three-phase asynchronous motors to measure the vibration signals of drive end bearing under different working conditions. The purpose of this study is to fulfill the fault feature extraction and states identification. Therefore, only the rolling bearing with 0.1788 mm single-point fault diameter are selected to be verified the proposed method.

In this experiment, the sample frequency and sample length are set to 12 kHz and 1200 point, respectively. The vibration signals of rolling bearing with four different bearing typical states (i.e., normal, IRF, ORF and BF) are collected by the acceleration sensor under different speeds and different loads, respectively. The speeds are 1730 r/min, 1750 r/min, 1772 r/min, and 1797 r/min, and the corresponding loads are 3 hp, 2 hp, 1 hp, and 0 hp. Table 2 is the selected experimental data in this paper. *A*, *B*, *C*, and *D* are used to represent four different operation conditions, respectively. For each operation condition, 200 samples are randomly selected (including 50 samples of each four typical state pieces), 800 samples are obtained in total, and each sample is 1200 points. The training data contains 480 samples and the testing data contains 320 samples.

5.2 Time-Frequency Analysis and Feature Extraction Method

5.2.1 Time-Frequency Analysis Based on GST

Taking operation condition *A* as an example, the time domain waveform of four different bearing typical states vibration signal are shown in Figure 5.

Table 2 Experimental data for bearing fault diagnosis

Working condition	Motor speed (r/min)	Motor loads (hp)	Normal		IRF		ORF		BF	
			Training	Test	Training	Test	Training	Test	Training	Test
A	1730	3	30	20	30	20	30	20	30	20
B	1750	2	30	20	30	20	30	20	30	20
C	1772	1	30	20	30	20	30	20	30	20
D	1797	0	30	20	30	20	30	20	30	20

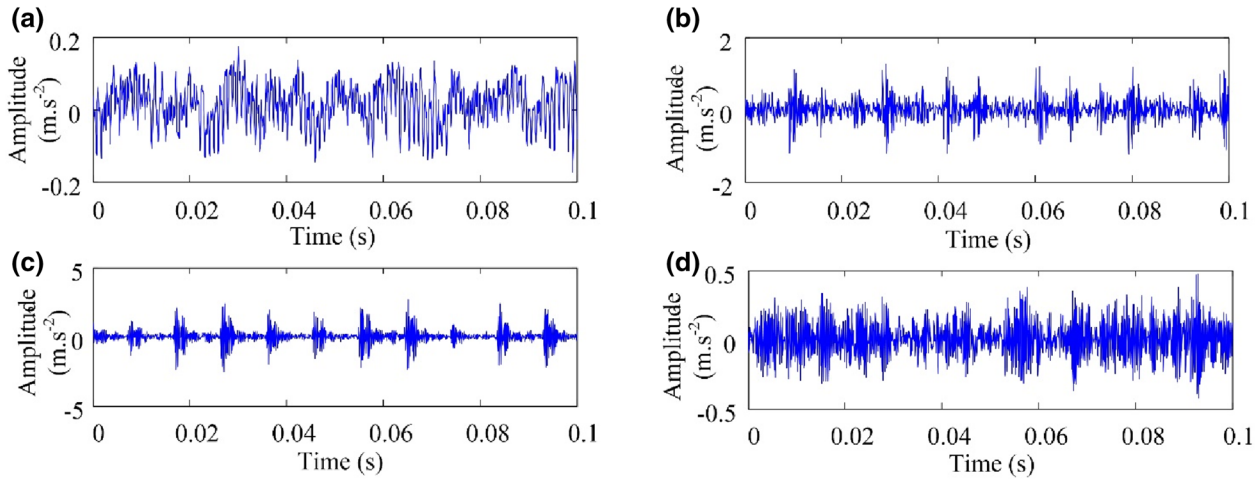

Figure 5 Time domain waveform of four different bearing typical states vibration signal: (**a**) normal, (**b**) IRF, (**c**) ORF, (**d**) BF

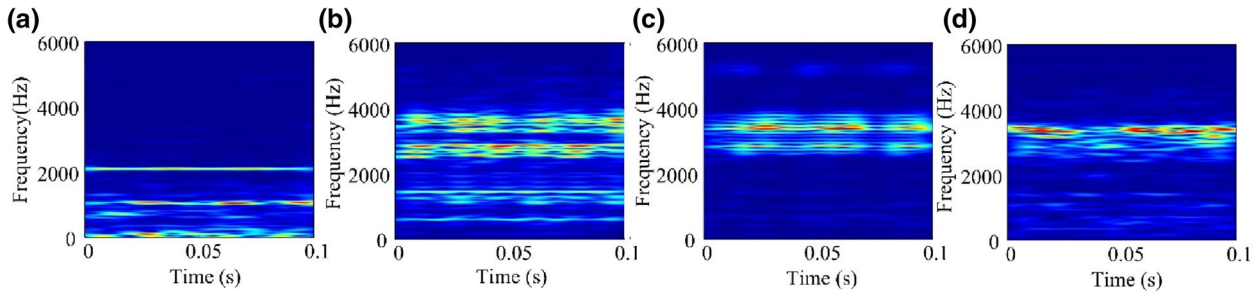

Figure 6 Time-frequency representation of raw signal using STFT: (**a**) normal, (**b**) IRF, (**c**) ORF, (**d**) BF

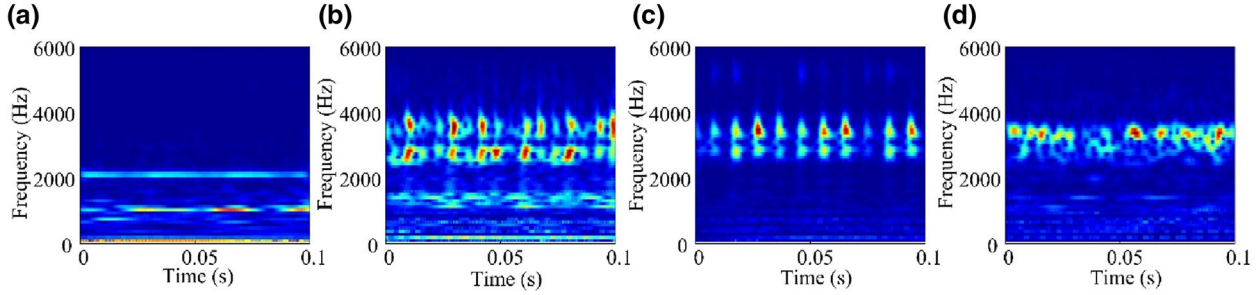

Figure 7 Time-frequency representation of raw signal using CWT: (**a**) normal, (**b**) IRF, (**c**) ORF, (**d**) BF

The time-frequency representation using STFT, CWT, standard S transform and optimal GST are displayed and compared in Figures 6, 7, 8 and 9.

As shown in Figure 6, the impact feature information caused by the fault of the rolling bearing is completely misrepresent due to the deficient time resolution of the STFT. As shown in Figure 7, although the impact feature information can be obtained from the time-frequency representation, the concentration of fault frequency component is very poor. The fault frequency component of the standard S transform has a good time domain resolution. However, its frequency-domain resolution is poor, as shown in Figure 8. As shown in Figure 9, after the raw signal is converted in the time-frequency domain

by using the optimal GST, the obtained time-frequency representation has good concentration in both the time domain and frequency-domain.

Therefore, the feature information of rolling bearing vibration signal obtained by optimal GST has the better time-frequency concentration than other time-frequency analysis methods.

5.2.2 Feature Extraction Based on GST and SVD

The amplitude matrix of the raw signal obtained by GST is used to the feature matrix. The singular values can be acquired by using SVD to the feature matrix and the results of four different bearing typical states are shown in Figure 10. Compared with results of standard S transform and SVD (as shown in Figure 11), the results obtained by GST and SVD are more coincident and stable.

In the present study, the operating states of rolling bearing include normal, IRF, ORF and BF. To observe the disparity of singular values in different operating states, the singular value clusters obtained by GST and SVD methods are shown in Figure 12(a). In order to observe the difference more clearly, the first 10 order singular values are compared, as shown in Figure 12(b).

As shown in Figure 12, the gaps between the different operating states are large enough and they can be easily distinguishable by using GST and SVD methods.

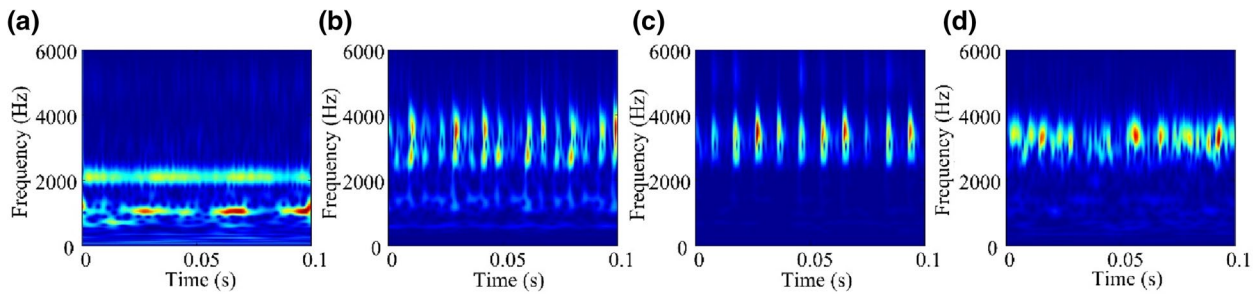

Figure 8 Time-frequency representation of raw signal using standard S transform: (**a**) normal, (**b**) IRF, (**c**) ORF, (**d**) BF

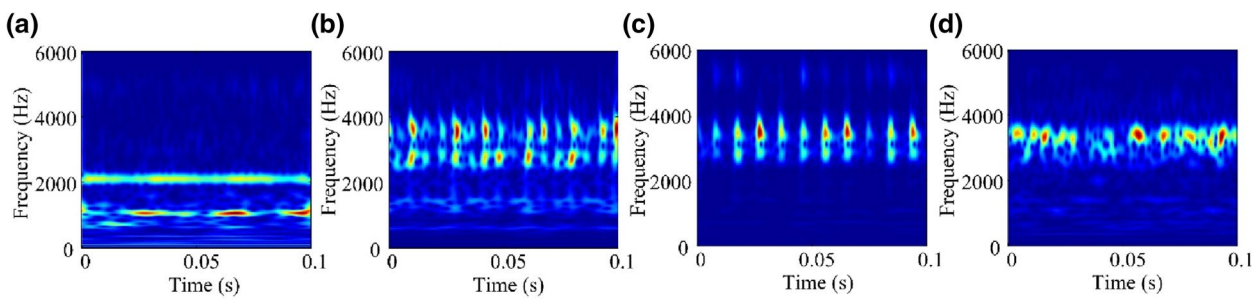

Figure 9 Time-frequency representation of raw signal using optimal GST: (**a**) normal, (**b**) IRF, (**c**) ORF, (**d**) BF

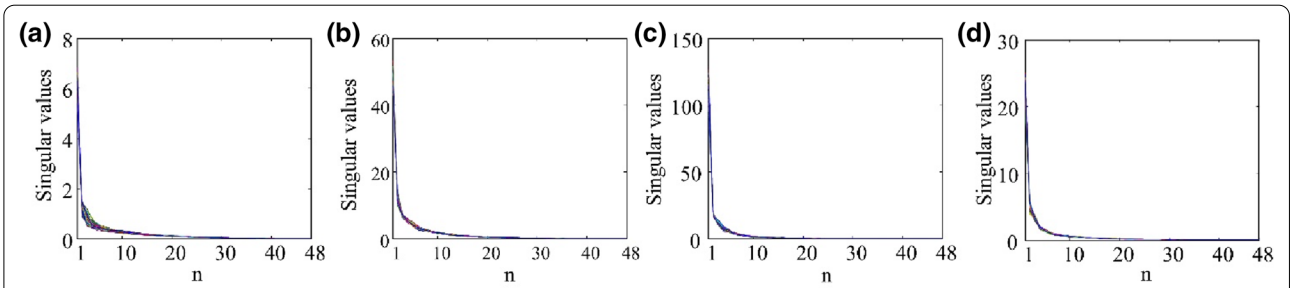

Figure 10 Singular values obtained by GST and SVD: (**a**) normal, (**b**) IRF, (**c**) ORF, (**d**) BF

In addition, in the example, the noise level of the vibration signals is relatively low, while in real-world application, tremendous noise level may corrupt the vibration signal. Therefore, the Gaussian white noise with a signal-to-noise ratio (SNR) of 5 dB is added to the experimental signal to simulate the engineering practice. The feature extraction result by GST and SVD methods is shown in Figure 13(a). In order to observe the difference more clearly, the first 10 order singular values are compared, as shown in Figure 13(b).

When the SNR of the signal is 5 dB, the extracted features are similar, and the gaps between the different operating states are large enough, as shown in Figure 13.

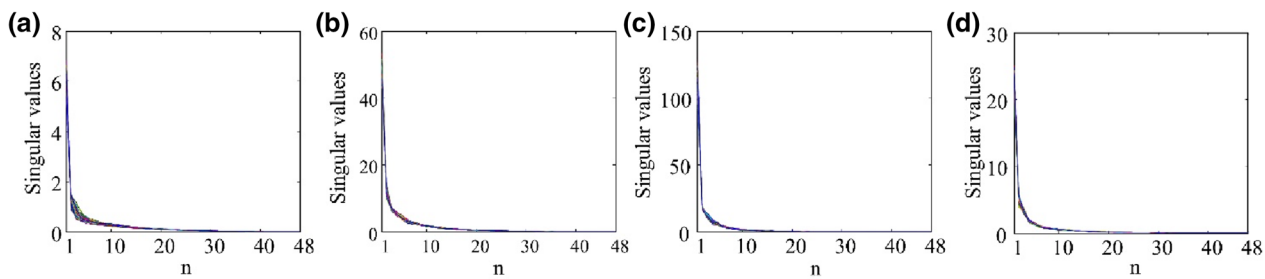

Figure 11 Singular values obtained by standard S transform and SVD: (**a**) normal, (**b**) IRF, (**c**) ORF, (**d**) BF

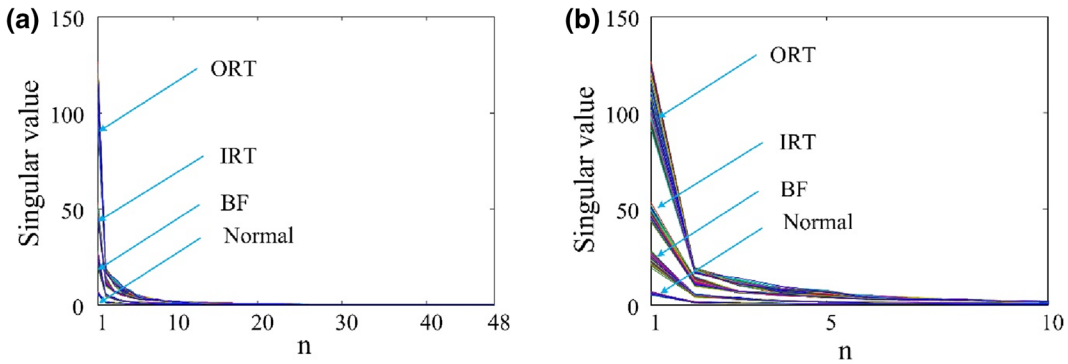

Figure 12 Singular value clusters for different operating states: (**a**) first 48 order; (**b**) first 10 order

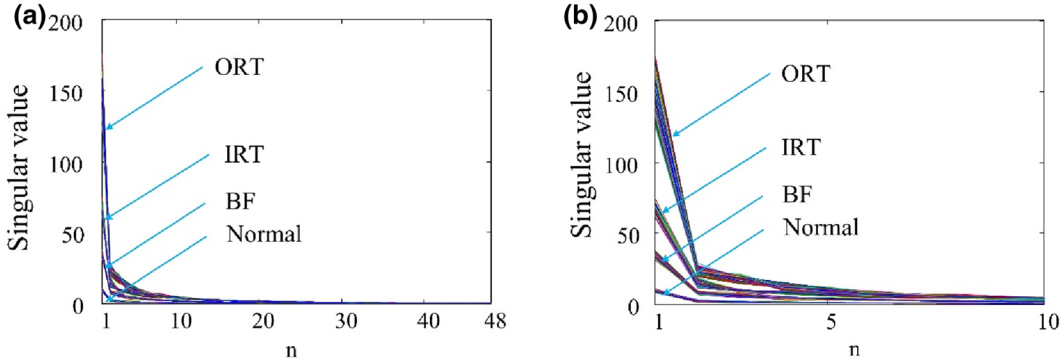

Figure 13 Feature extraction result by GST and SVD methods: (**a**) first 48 order; (**b**) first 10 order

5.2.3 Data Compression for the Feature Vectors Based on PCA Method

The feature vector is composed of 48 feature quantities of singular values, as shown in Figure 10. When using the intelligent algorithms to identify the different faults states, the excessive feature quantities will train more complex models and reduce the learning speed of training data [25]. To solve the problem, PCA is introduced in this study. The PCA is used to reduce and optimize the feature matrix, which composed of multiple sets of singular value vectors. The feature parameters extracted by PCA are used as the input of intelligent algorithm model in this study.

To ensure the identification accuracy of different faults states of rolling bearing under variable operation conditions, the training data are taken as an example. Principal component analysis (PCA) is an effective data dimensionality reduction algorithm. In this paper, the PCA is used to reduce and optimize the feature matrix, which composed of multiple sets of singular value vectors. Firstly, the feature matrix is normalized. Secondly, the covariance of each principal component in the normalized characteristic matrix is calculated. The ratio of principal component covariance to the sum of all principal component covariance is defined as the principal component contribution. Finally, the principal components with cumulative contribution rate higher than 95% are selected as the feature vectors of the condition components. The selected principal component contribution rate is shown in Table 3 (limited to space, only listed the cumulative contribution rate is higher than 95% of the principal component).

Table 3 The cumulative contribution rate of the principal component

The principal component	Singular value	Contribution rate (%)	Cumulative contribution rate (%)
1	41.2185	87.9	87.9
2	2.8704	6.12	94.02
3	0.8897	1.9	95.92

According to Table 3, the first three principal components are extracted as simplified feature parameters. Figure 14 is a feature waveform of the first three principal components after fusion using the PCA method.

As shown in Figure 14, the first-order principal component and second-order principal component retains most of the information of the raw signal, and the change trend of the bearings in different bearing typical states are represented well. The change trend is basically consistent with the sample states. The third-order principal components more chaotic overall, and the ability to characterize bearings in different states is weak. The circles in Figure 14(a, b) are correspond to four typical states of rolling bearing, respectively.

5.3 State Classification Based on PSO-SVM

5.3.1 The Proposed Method

The feature parameters extracted by GST and SVD-PCA are used as the input of PSO-SVM model. The main parameters of PSO are set as: particle population size is 20, the maximum number of iterations is 100, and learning factors are set as c_1=1.5 and c_2=1.7. The PSO is used to optimize the SVM model, and the optimal penalty factor and kernel function parameters are obtained as 16.7647 and 2.28269, respectively. Labels 1 to 4 indicate four different typical states of the bearing, respectively. State classification results of training data and testing data based on PSO-SVM are shown in Figure 15. As a comparison, the state classification results using PSO-SVM based on GST and SVD are shown in Figure 16.

As shown in Figure 15, we can see that even under variable conditions, the training data and testing data actual

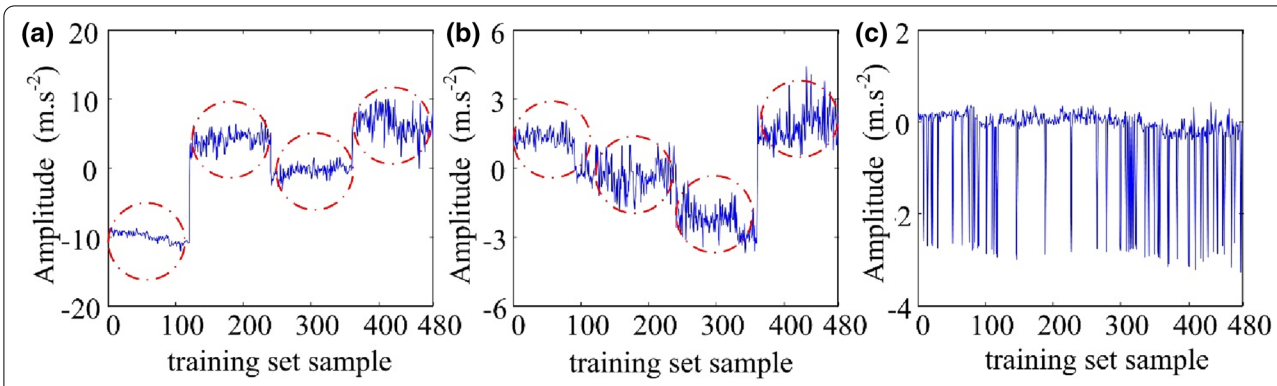

Figure 14 Trend of the first three-order principal components of the training set sample: (**a**) first-order principal component, (**b**) second-order principal component, (**c**) third-order principal component

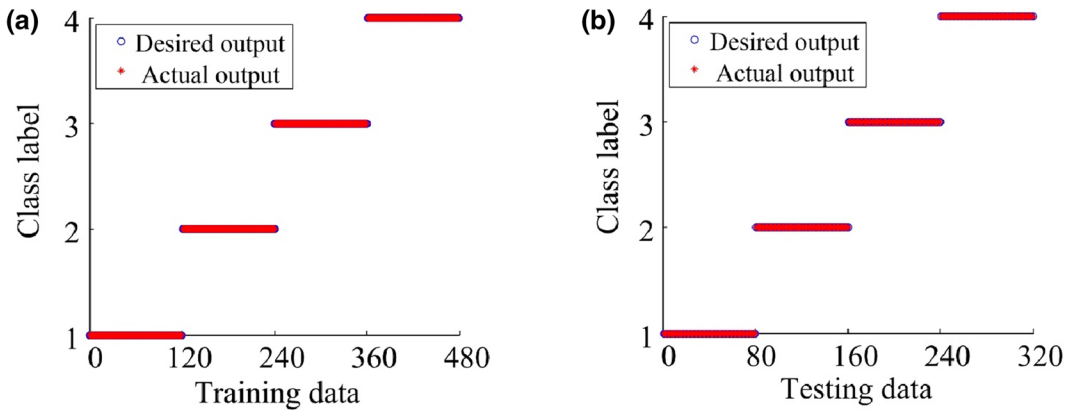

Figure 15 State classification results using PSO-SVM based on GST and SVD-PCA: (**a**) training data, (**b**) testing data

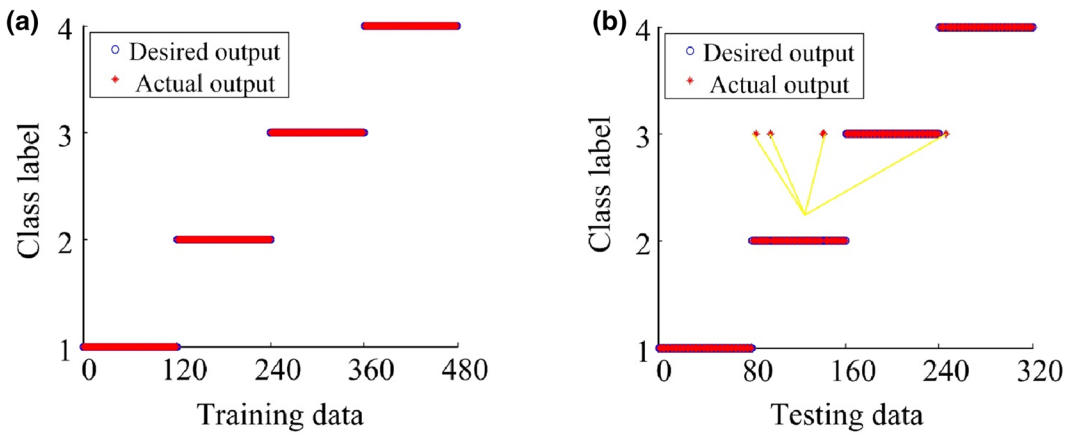

Figure 16 State classification results using PSO-SVM based on GST and SVD: (**a**) training data, (**b**) testing data

output of PSO-SVM are consistent with the desired output. The errors of state classification results using the proposed method are calculated to be zero. As shown in Figure 16, the training data actual outputs errors of PSO-SVM are calculated to be zero, however the testing data actual outputs errors are 1.25%. In other words, The PCA can reduce and optimize the singular value vectors matrix, and obtained a simplified PSO-SVM model. Thus, the proposed method using PSO-SVM based on GST and SVD-PCA is able to efficiently realize the fault diagnosis of rolling bearing under variable conditions.

5.3.2 Comparison of Recognition Accuracy with Different Feature Extraction Methods

In order to verify the superiority and effectiveness of the proposed method for rolling bearing fault diagnosis, the PSO-SVM model with different feature extraction methods are employed for comparison. The feature extraction methods are list as follows:

(1) Standard S transform and SVD methods: The S transform is used to conduct a time-frequency transformation for a raw signal. Subsequently, the two-dimensional complex matrix can be obtained. Then, the SVD is performed to the matrix to obtain the feature vectors.
(2) Local mode decomposition (LMD) and SVD methods: The raw signal is decomposed by LMD method. Subsequently, several product functions (PFs) component can be obtained. Then, the SVD is performed to the PF component to obtain the feature vectors [24].
(3) Wavelet approximation entropy method: Based on the DB5 wavelet basis, the fault vibration signal of rolling bearing is decomposed by four layers of wavelet. The feature vectors are obtained by calculate the approximate entropy of each layer frequency band [37].

Table 4 Classification result comparison among different classification algorithms

Different feature extraction method	Model	Classification accuracy Training data	Testing data	Running time (s) Training data	Testing data
Standard S transform	PSO-SVM	1	0.9444	7.752	5.606
	BP	0.9854	0.9000	8.351	6.936
LMD and SVD	PSO-SVM	1	0.9861	6.608	4.652
	BP	0.9896	0.9667	7.021	5.654
Wavelet approximation entropy	PSO-SVM	1	0.9722	6.608	4.652
	BP	0.9875	0.9639	8.021	6.654
GST-SVD-PCA	**PSO-SVM**	**1**	**1**	**5.687**	**4.553**
	BP	0.9958	0.9694	6.008	5.583

Bold values indicate the results obtained using the proposed method

Moreover, a typical example of neural networks named Back Propagation (BP) is also applied. The state classification results of different models with different feature extraction methods are listed in Table 4.

It can be seen from Table 4, compared with the same feature extraction method, although the PSO-SVM model has more time-consuming, it has an obviously higher accurate classification and efficiency than BP model. In addition, compared with the same model, the feature extraction method based on GST and SVD-PCA methods has an obvious superiority over other methods. The results indicate that the extracted feature parameters are more effective by the proposed method, which can be used as input to the intelligent model to obtain higher recognition accuracy.

In a word, the accuracy of different bearing typical states classification and identification can be effectively improved by the proposed method.

6 Conclusions

In this paper a feasibility study of a time-frequency analysis methodology, based on the GST and SVD applied to fault feature extraction problems in rolling bearing under variable conditions, has been analyzed. In addition, the PCA is subsequently performed to the feature vectors to extract the more streamlined feature parameters for accurate fault classification. The fault states are identified and classified by PSO-SVM model. A detailed comparison is made among STFT, CWT and GST methods. The results show that the GST method can obtain a more satisfactory time frequency representation than other similar techniques. Furthermore, a detailed comparison is made between standard S transform-SVD and GST -SVD. The results shows that the GST-SVD are more coincident and stable than standard S transform-SVD method. The experimental data analysis indicate that the proposed method could effectively extract the feature parameters of rolling bearing under variable conditions.

Acknowledgements
Not applicable.

Authors' Contributions
XL was in charge of the whole trail and wrote the manuscript; XZ assisted with sampling and laboratory analyses. KF modified the manuscript to improve the presentation. All authors read and approved the final manuscript.

Authors' Information
Xiangnan Liu, born in 1992, is currently a PhD candidate in mechanical engineering at Department of Mechanical and Automotive Engineering, South China University of Technology, China, in 2019. His main research interests include dynamic monitoring and diagnosis of mechanical systems.
Xuezhi Zhao, born in 1970, is currently a full professor at Department of Mechanical and Automotive Engineering, South China University of Technology, China, in 2011. His main research interests include dynamic monitoring and diagnosis of mechanical systems, signal processing, and singular value decomposition.
Kuanfang He, born in 1979, is currently a full professor at School of Mechatronic Engineering and Automation, Foshan University, Foshan; China, in 2019. His main research interests include design theory and applications of On-line monitoring of welding cracks.

Funding
Supported by Guangdong Provincial Natural Science Foundation of China (Grant No. 2020B1515120006), Guangdong Innovation Team (Grant Nos. 2020KCXTD015, 2022KCXTD029) and Guangdong Universities New Information Field (Grant No. 2021ZDZX1057).

Competing Interests
The authors declare that they have no competing interests.

Author Details
[1]School of Mechanical and Automotive Engineering, South China University of Technology, Guangzhou 510641, China. [2]School of Mechatronic Engineering and Automation, Foshan University, Foshan 528225, China.

Received: 30 September 2022 Revised: 30 September 2022 Accepted: 9 October 2022
Published online: 03 November 2022

References

[1] S Gao, Q Wang, Y Zhang. Rolling bearing fault diagnosis based on CEEMDAN and refined composite multiscale fuzzy entropy. *IEEE Transactions on Instrumentation and Measurement*, 2021, 70: 1-8.
[2] Y Zhou, S Yan, Y Ren, et al. Rolling bearing fault diagnosis using transient-extracting transform and linear discriminant analysis. *Measurement*, 2021, 178: 109298.

[3] J Cheng, Y Yang, X Li, et al. Adaptive periodic mode decomposition and its application in rolling bearing fault diagnosis. *Mechanical Systems and Signal Processing*, 2021, 161: 107943.
[4] J Zheng, H Pan, S Yang, et al. Generalized composite multiscale permutation entropy and Laplacian score based rolling bearing fault diagnosis. *Mechanical Systems and Signal Processing*, 2018, 99: 229-243.
[5] Y Tian, J Ma, C Lu, et al. Rolling bearing fault diagnosis under variable conditions using LMD-SVD and extreme learning machine. *Mechanism and Machine Theory*, 2015, 90: 175-186.
[6] M Qiao, S Yan, X Tang, et al. Deep convolutional and LSTM recurrent neural networks for rolling bearing fault diagnosis under strong noises and variable loads. *IEEE Access*, 2020, 8: 66257-66269.
[7] H Su, L Xiang, A Hu, et al. A novel hybrid method based on KELM with SAPSO for fault diagnosis of rolling bearing under variable operating conditions. *Measurement*, 2021, 177: 109276.
[8] M Li, J Yang, X Wang. Fault feature extraction of rolling bearing based on an improved cyclical spectrum density method. *Chinese Journal of Mechanical Engineering*, 2015, 28(6): 1240-1247.
[9] X Li, Z Ma, D Kang, X Li. Fault diagnosis for rolling bearing based on VMD-FRFT. *Measurement*, 2020, 155: 107554.
[10] Y Xu, Z Li, S Wang, et al. A hybrid deep-learning model for fault diagnosis of rolling bearings. *Measurement*, 2021, 169: 108502.
[11] M Singh, A G Shaik. Incipient fault detection in stator windings of an induction motor using stockwell transform and SVM. *IEEE Transactions on Instrumentation and Measurement*, 2020, 69(12): 9496-9504.
[12] Y J Shin, E J Powers, T S Choe, et al. Application of time-frequency domain reflectometry for detection and localization of a fault on a coaxial cable. *IEEE Transactions on Instrumentation and Measurement*, 2005, 54(6): 2493-2500.
[13] X Ding, Q He. Energy-fluctuated multiscale feature learning with deep convnet for intelligent spindle bearing fault diagnosis. *IEEE Transactions on Instrumentation and Measurement*, 2017, 66(8): 1926-1935.
[14] R Yan, R X Gao. Energy-based feature extraction for defect diagnosis in rotary machines. *IEEE Transactions on Instrumentation and Measurement*, 2009, 58(9): 3130-3139.
[15] J Yu, H Liu. Sparse coding shrinkage in intrinsic time-scale decomposition for weak fault feature extraction of bearings. *IEEE Transactions on Instrumentation and Measurement*, 2018, 67(7): 1579-1592.
[16] R G Stockwell, L Mansinha, R P Lowe. Localization of the complex spectrum: The S transform. *IEEE Transactions on Signal Processing*, 1996, 44(4): 998-1001.
[17] Z Wang, L Yao, G Chen, et al. Modified multiscale weighted permutation entropy and optimized support vector machine method for rolling bearing fault diagnosis with complex signals. *ISA Transactions*, 2021, 114: 470-484.
[18] S Chatterjee, N R Choudhury, R Bose. Detection of epileptic seizure and seizure-free EEG signals employing generalised S-transform. *IET Science, Measurement & Technology*, 2017, 11(7): 847-855.
[19] P D McFadden, J G Cook, L M Forster. Decomposition of gear vibration signals by the generalised S transform. *Mechanical Systems and Signal Processing*, 1999, 13(5): 691-707.
[20] Z Wei, Y Mao, Z Yin, et al. Fault detection based on the generalized S-Transform with a variable factor for resonant grounding distribution networks. *IEEE Access*, 2020, 8: 91351-91367.
[21] C R Pinnegar. The generalized S-transform and TT-transform, in one and two dimensions. *International Journal of Oral & Maxillofacial Surgery*, 2002, 38(6): 422.
[22] B Wang, S L Liu, H L Zhang. Fault feature extraction for rolling bearings based on generalized S transformation optimized with Quantum genetic algorithm. *Journal of Vibration & Shock*, 2017, 36(5): 108-113.
[23] Z Feng, X Chen, T Wang. Time-varying demodulation analysis for rolling bearing fault diagnosis under variable speed conditions. *Journal of Sound and Vibration*, 2017, 400: 71-85.
[24] M Pogačar, G Čepon, M Boltežar. Weakening of the multi-point constraints in modal substructuring using singular value decomposition. *Mechanical Systems and Signal Processing*, 2022, 163: 108109.
[25] F Guo, H Gao, Z Wang, et al. Feature extraction method of series fault arc based on ST-SVD-PCA. *Journal of China Coal Society*, 2018, 43(3): 888-896.
[26] W Zou, D Froning, Y Shi, et al. A least-squares support vector machine method for modeling transient voltage in polymer electrolyte fuel cells. *Applied Energy*, 2020, 271: 115092.
[27] W Jiang, Y Xie, W Li, et al. Prediction of the splitting tensile strength of the bonding interface by combining the support vector machine with the particle swarm optimization algorithm. *Engineering Structures*, 2021, 230: 111696.
[28] Y-W Wang, H-Q Yang, P Zhang. Iterative convergence control method for planar underactuated manipulator based on support vector regression model. *Nonlinear Dynamics*, 2020, 102(4): 2711-2724.
[29] I Djurović, E Sejdić, J Jiang. Frequency-based window width optimization for S-transform. *AEU-International Journal of Electronics and Communications*, 2008, 62(4): 245-250.
[30] L Stanković. A measure of some time–frequency distributions concentration. *Signal Processing*, 2001, 81(3): 621-631.
[31] X Zhao, B Ye. Selection of effective singular values using difference spectrum and its application to fault diagnosis of headstock. *Mechanical Systems and Signal Processing*, 2011, 25(5): 1617-1631.
[32] K He, X Liu, Q Yang, et al. An extraction method of welding crack acoustic emission signal using harmonic analysis. *Measurement*, 2017, 103: 311-320.
[33] H Wang, G Ni, J Chen, et al. Research on rolling bearing state health monitoring and life prediction based on PCA and Internet of Things with multi-sensor. *Measurement*, 2020, 157(4): 107657.
[34] S Dong, T Luo. Bearing degradation process prediction based on the PCA and optimized LS-SVM model. *Measurement*, 2013, 46(9): 3143-3152.
[35] W A Smith, R B Randall. Rolling element bearing diagnostics using the Case Western Reserve University data: A benchmark study. *Mechanical Systems and Signal Processing*, 2015, 64: 100-131.
[36] X Li, J Ma, X Wang, et al. An improved local mean decomposition method based on improved composite interpolation envelope and its application in bearing fault feature extraction. *ISA Transactions*, 2020, 97: 365-383.
[37] L-Y Zhao, L Wang, R-Q Yan. Rolling bearing fault diagnosis based on wavelet packet decomposition and multi-scale permutation entropy. *Entropy*, 2015, 17(9): 6447-6461.